Lidar-measured atmospheric N_2 vibrational-rotational Raman spectra and consequent temperature retrieval

Fuchao Liu[1, 2] and Fan Yi[1, 2, *]

[1]*School of Electronic Information, Wuhan University, Wuhan 430072, China*
[2] *State Key Laboratory of Information Engineering in Surveying, Mapping and Remote Sensing, Wuhan University, Wuhan 430079, China*
[*] *yf@whu.edu.cn*

Abstract: We have built a spectrally resolved Raman lidar to measure atmospheric N_2 Stokes vibrational-rotational Raman spectra. The lidar applies a double-grating polychromator with a reciprocal linear dispersion of ~0.12 nm mm^{-1} for the wavelength separation and a 32-channel linear-array photomultiplier tube for sampling the spectral signals. The lidar can together measure the individual S- and O-branch line signals from J = 0 (2) through 14 (16). A comparison shows an excellent agreement between the lidar-measured and theoretically-calculated spectra. Based on the signal ratio of two individual lines (e.g., S-branch J = 6 and 12), the atmospheric temperature profiles are derived without requiring a calibration from another reference temperature. In terms of the envelope shape of an even-J section of the measured S-branch lines, we have also developed a new temperature retrieval approach without needing a calibration from reference temperature data. Both the approaches can give rise to reasonable temperature profiles comparable to that from local radiosonde.

OCIS codes: (010.0010) Atmospheric and oceanic optics; (120.0280) Remote sensing and sensors; (120.6780) Temperature; (280.3640) Lidar.

References and links

1. Y. F. Arshinov, S. M. Bobrovnikov, V. E. Zuev, and V. M. Mitev, "Atmospheric temperature measurements using a pure rotational Raman lidar," Appl. Opt. **22**(19), 2984–2990 (1983).
2. Y. Arshinov, S. Bobrovnikov, I. Serikov, A. Ansmann, U. Wandinger, D. Althausen, I. Mattis, and D. Müller, "Daytime operation of a pure rotational Raman lidar by use of a Fabry-Perot interferometer," Appl. Opt. **44**(17), 3593–3603 (2005).
3. J. Reichardt, "Cloud and aerosol spectroscopy with Raman lidar," J. Atmos. Ocean. Technol. **31**(9), 1946–1963 (2014).
4. D. Nedeljkovic, A. Hauchecorne, and M. L. Chanin, "Rotational Raman lidar to measure the atmospheric temperature from the ground to 30 km," IEEE Trans. Geosci. Rem. Sens. **31**(1), 90–101 (1993).
5. A. Behrendt, Temperature measurement with Lidar, in *Lidar Range-Resolved Optical Remote Sensing of the Atmosphere* (C. Weitkamp, 2005), Chap. 10.
6. U. Wandinger, Raman lidar, in *Lidar Range-Resolved Optical Remote Sensing of the Atmosphere* (C. Weitkamp, 2005), Chap. 9.
7. F. C. Liu and F. Yi, "Spectrally resolved Raman lidar measurements of gaseous and liquid water in the atmosphere," Appl. Opt. **52**(28), 6884–6895 (2013).
8. F. Yi, S. D. Zhang, C. M. Yu, Y. J. He, X. C. Yue, C. M. Huang, and J. Zhou, "Simultaneous observations of sporadic Fe and Na layers by two closely colocated resonance fluorescence lidars at Wuhan (30.5°N, 114.4°E), China," J. Geophys. Res. **112**(D4), D04303 (2007).

1. Introduction

When a narrow-linewidth (typically ~0.003 cm^{-1}) laser light propagates in atmosphere, the irradiated atmospheric molecules (mainly N_2, O_2 and H_2O) emit the secondary radiations via the elastic and inelastic scattering. The elastically scattered radiation that has nearly the same

#222826 - $15.00 USD Received 11 Sep 2014; revised 13 Oct 2014; accepted 20 Oct 2014; published 3 Nov 2014

frequency as the incident light is designated "Cabannes line" which represents a collective effect from all kinds of atmospheric molecules. It has a Voigt line shape (FWHM ~0.1 cm^{-1}), exhibiting the broadening by the temperature, pressure and bulk motion of the molecules. The inelastically scattered radiation, whose frequency is shifted from that of the incident light, is composed of the pure rotational Raman (PRR) band and vibrational-rotational Raman (VRR) bands. The PRR band consists of the Stokes (red-shifted) and anti-Stokes (blue-shifted) rotational Raman lines distributed on the two nearby sides (extending ~200 cm^{-1} either side) of the Cabannes line. The joint contribution from the atmospheric N_2 and O_2 molecules makes the rotational Raman lines more compact in spacing than that induced by N_2 or O_2 molecule alone. This makes it hard to extract individual PRR lines with the existing lidar spectral extraction devices. The VRR bands are far from the Cabannes line. They comprise the Stokes (red-shifted) VRR bands and anti-Stokes (blue-shifted) ones. Since the anti-Stokes VRR bands are in intensity several orders weaker than the corresponding Stokes bands, only the Stokes VRR bands are usually used for the Raman measurement of atmosphere. The clear-cut wavelength separation of the VRR bands for the different molecular species (e.g., N_2, O_2 and H_2O) allows their concentrations to be measured by lidar. The (Stokes) VRR band for each molecular species contains three branches of spectral lines. One is called the Q branch. It refers to the dense and strong central lines that are too closely spaced to be resolved by the existing Raman lidars. The Raman lidar measurement of concentration for a given molecular species is made actually via extracting the Q-branch signal. Another two are the wing lines to the sides of the Q branch, called the O and S branches respectively. Although the intensities of the VRR lines in the O and S branches is usually 2-3 orders of magnitude smaller than that of the corresponding PRR lines, their relatively-wide and nearly-invariable line spacing allows the individual VRR lines to be extracted by lidar.

As a result of the population distribution of molecular rotational energy levels, the intensity of a single PRR line is a simple function of temperature. Thus the ratio of the lidar-detected signals from two individual PRR lines exactly has a temperature dependence defined by the Boltzmann distribution [1]. This gives conceptually the basic principle for a PRR lidar to measure atmospheric temperature profiles. Since the N_2 and O_2 PRR lines intermingle in a narrow spectral region (~10 nm), it is challenging to pick out individual N_2 or O_2 PRR lines except for Raman lidars with extremely high spectral resolution [2, 3]. For the most existing PRR lidars, each Raman channel usually extracts several adjacent N_2 and O_2 PRR lines rather than a single one. In this instance, for the reduction of the temperature measurement error due to the multiple PRR lines extraction, a modified calibration function (a second-order polynomial function of inverse temperature) needs to introduce [4, 5].

As a primary and steady atmospheric constituent, the N_2 molecule is appropriate to act as a Raman scatterer for the temperature measurement. The Stokes VRR lines of N_2 are widely separate from that of other molecular species and their wing lines spacing is moderately large (for example, when the lidar emits a radiation at 354.8 nm, the resultant atmospheric N_2 VRR wing lines have a line spacing of ~0.12 nm). The features make it feasible to extract individual N_2 VRR lines. Note that the intensity of a single N_2 VRR O- or S-branch line has similar temperature dependence to the corresponding N_2 PRR line [6]. Thus the atmospheric temperature profiles can also be derived from the signal ratio of two lidar-detected individual N_2 VRR lines (in the O or S branch) based on the strict Boltzmann temperature dependence. In addition, as the N_2 VRR lines are far from the Cabannes line, it is relatively easier to suppress the elastically scattered light in the Raman channels.

A spectrally resolved Raman (SRR) lidar has been built to measure atmospheric N_2 Stokes VRR spectra. The groundwork for this development has already been laid via our previous work on the spectrally resolved water Raman lidar [7] and resonance fluorescence lidar [8]. The SRR lidar can simultaneously extract the individual N_2 VRR lines of S branch from $J = 0$ through 14 and O branch from $J = 2$ through 16. This allows the atmospheric temperature profiles to be retrieved in terms of the strict Boltzmann temperature dependence. In addition,

#222826 - $15.00 USD Received 11 Sep 2014; revised 13 Oct 2014; accepted 20 Oct 2014; published 3 Nov 2014

based on the envelope shape of the N_2 Stokes VRR lines of S branch measured by the lidar, we have developed a new method for deriving temperature profiles without need of calibration from reference temperature data.

2. N_2 vibrational-rotational Raman spectra and lidar equation

For the purpose of designing a spectrally resolved N_2 Raman lidar, we first revisit some concepts on the N_2 Stokes VRR band in which the vibrational quantum number v changes from 0 to 1 ($v = 0 \rightarrow 1$) [6]. In terms of the selection rules, the N_2 Stokes VRR band consists of three spectral line branches corresponding to three different changes in the rotational quantum number J. The line group with a change of $\Delta J = 0$ is designated "Q" branch, while another two wing line groups with changes of $\Delta J = +2$ and $\Delta J = -2$ are called "S" and "O" branches, respectively. The Raman backscatter cross section depicts quantitatively the characteristics of the Raman spectra. At the absolute temperature T, the differential backscattering cross section for a single N_2 Stokes VRR line excited by an emission at a frequency (wavenumber) $\tilde{\nu}_0$ can be expressed as [6]:

$$\begin{cases} \sigma^i(J,T) = (2\pi)^4 \cdot [\tilde{\nu}_0 - |\Delta\tilde{\nu}(J)|^i]^4 \cdot \dfrac{g_N \cdot \Phi^i(J)}{(2I_N+1)^2 \cdot Q} \cdot \exp[-\dfrac{hcB_0 \cdot J(J+1)}{kT}], \\ i = S \text{ and } Q: \ J = 0,1,2,...; \quad i = O: \ J = 2,3,4,..., \end{cases} \tag{1}$$

where h is Planck's constant, c the velocity of light, B_0 (= 1.98957 cm^{-1}) the N_2 rotational constant corresponding to $v = 0$, k the Boltzmann constant, I_N (= 1) the nuclear spin. g_N is the statistical weight factor whose value is 6 and 3 respectively for even and odd J. $Q \approx kT/(2hcB_0)$ is the partition function. $\Delta\tilde{\nu}(J)$ denotes the Raman frequency shift amount for the line. For those spectral lines with J less than 22, the frequency shift can be well approximated as:

$$|\Delta\tilde{\nu}(J)|^S \approx \tilde{\nu}_{vib} + (4J+6)B_1, \ J = 0,1,2,..., \tag{2.1}$$

$$|\Delta\tilde{\nu}(J)|^Q \approx \tilde{\nu}_{vib} + J(J+1)(B_1 - B_0), \ J = 0,1,2,..., \tag{2.2}$$

$$|\Delta\tilde{\nu}(J)|^O \approx \tilde{\nu}_{vib} - (4J-2)B_0, \ J = 2,3,4,..., \tag{2.3}$$

where $\tilde{\nu}_{vib}$ (= 2330.7 cm^{-1}) is the N_2 specific vibrational wavenumber, and B_1 (= 1.97219 cm^{-1}) the N_2 rotational constant corresponding to $v = 1$. The function $\Phi(J)$ is given by:

$$\Phi^S(J) = \frac{h}{8\pi^2 c\tilde{\nu}_{vib} \cdot [1 - \exp(-hc\tilde{\nu}_{vib}/kT)]} \cdot \frac{7(J+1)(J+2)}{30(2J+3)} \gamma'^2, \ J = 0,1,2,..., \tag{3.1}$$

$$\Phi^Q(J) = \frac{h \cdot (2J+1)}{8\pi^2 c\tilde{\nu}_{vib} \cdot [1 - \exp(-hc\tilde{\nu}_{vib}/kT)]} \cdot [\alpha'^2 + \frac{7(J+1)(J+2)}{45(2J-1)(2J+3)} \gamma'^2], \ J = 0,1,2,..., \tag{3.2}$$

$$\Phi^O(J) = \frac{h}{8\pi^2 c\tilde{\nu}_{vib} \cdot [1 - \exp(-hc\tilde{\nu}_{vib}/kT)]} \cdot \frac{7J(J-1)}{30(2J-1)} \gamma'^2, \ J = 2,3,4,..., \tag{3.3}$$

where α'^2 and γ'^2 are the constants related with the molecular polarizability tensor (α'^2 = 2.62×10^{-14} m^4 kg^{-1} and $\gamma'^2 = 4.23 \times 10^{-14}$ m^4 kg^{-1}).

#222826 - $15.00 USD Received 11 Sep 2014; revised 13 Oct 2014; accepted 20 Oct 2014; published 3 Nov 2014

From Eqs. (1)-(3), we have calculated at two different temperatures (200 and 300 K) the N_2 Stokes VRR spectra shown in Fig. 1 for an incident laser wavelength of 354.8 nm. As seen from Fig. 1, the Q-branch lines start at the frequency shift of $\tilde{\nu}_{vib}$ (2330.7 cm^{-1}, at a wavelength of ~386.8 nm) and extend only ~20 cm^{-1} (~0.3 nm) in the direction of high frequency. Obviously, the line spacing of the Q-branch lines is too small to be resolved by conventional lidar technique. The S- and O-branch lines are distributed on both sides of the Q branch with each branch extending ~200 cm^{-1}. The spacing from the Q-branch line $J = 0$ is ~11.83 cm^{-1} to the S-branch line $J = 0$ and ~11.93 cm^{-1} to the O-branch line $J = 2$, respectively. The "invasion" of the Q-branch lines affects the O branch only up to $J = 3$. The line spacing inside the S or O branches has nearly the same values (~7.89 cm^{-1} for the S branch and ~7.96 cm^{-1} for the O branch) from $J = 0$ (2) to 19 (21) that are equivalent to ~0.12 nm for the 354.8-nm incident light. Hence, a lidar with a spectral resolution of 0.12 nm is capable of extracting the individual S- and O-branch lines. In order to measure the main part of the S- and O-branch spectra, the designed Raman lidar needs to have a spectral coverage of ~4.0 nm.

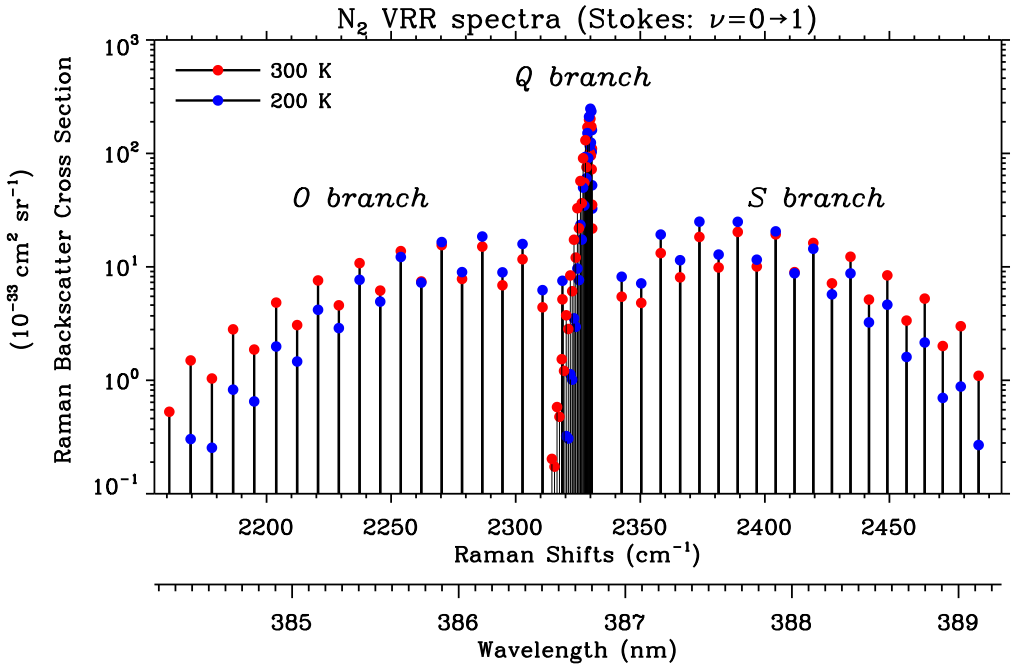

Fig. 1. The Stokes vibrational-rotational Raman (VRR) spectra of atmospheric N_2 obtained from a theoretical calculation for temperatures of 200 K (blue) and 300 K (red) respectively. The incident laser wavelength is 354.8 nm. Note that the S- and O-branch lines have nearly the same line spacing (~0.12 nm) from $J = 0$ (2) to 20.

The lidar equation for extracting individual N_2 VRR lines in the S and O branches has the following form (background subtracted):

$$N\left(\nu_J^i, z\right) = P_0 \frac{KO(z)}{z^2} H\left(\nu_J^i\right) n(z) \sigma^i(J,T) \tau\left(\tilde{\nu}_0\right) \tau\left(\nu_J^i\right). \quad (4)$$

Here $N\left(\nu_J^i, z\right)$ is the lidar-detected backscattered photon count of a single N_2 Stokes VRR line at frequency $\nu_J^i = \tilde{\nu}_0 - \left|\Delta\tilde{\nu}(J)\right|^i$ from distance z. P_0 is the transmitted laser power. K is

#222826 - $15.00 USD Received 11 Sep 2014; revised 13 Oct 2014; accepted 20 Oct 2014; published 3 Nov 2014

a frequency-independent system constant. $O(z)$ is the system overlap factor. $H(\nu_J^i)$ is the filter-function-related transmission of the receiver at line ν_J^i. $n(z)$ is the number density of N_2 molecules. $\tau(\tilde{\nu}_0)$ and $\tau(\nu_J^i)$ are the atmospheric transmissions for the incident line and the N_2 Stokes VRR line.

3. Lidar setup

Figure 2 gives the optical layout of the SRR lidar. The lidar transmitter employs an injection-seeded Nd:YAG laser (Spectra Physics, US) to emit an radiation of ~300 mJ per

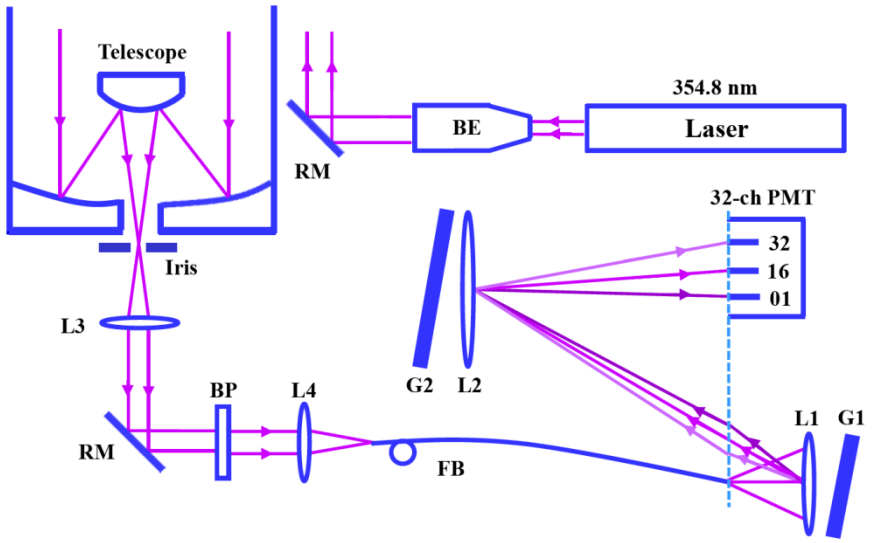

Fig. 2. Optical layout of the spectrally resolved N_2 vibrational-rotational Raman lidar for atmospheric temperature measurement. BE, beam expander; RM, reflecting mirror; L, lens; G, grating; BP, band pass filter; FB, fiber bundle; PMT, photomultiplier tube.

pulse at 354.8 nm with a 30 Hz repetition and 8 ns pulse width. A 5 × beam expander is equipped to reduce the divergence of the outgoing beam to ~0.1 mrad. A reflecting mirror is used to transmit the light into the atmosphere zenithward. The backscattered photons are collected by a 1-m Cassegrain telescope (focal length = 8 m). The subsequent optics contains a field-stop iris and collimating lens. The light exiting the collimating lens is redirected and then passes through a bandpass filter (Semrock, US) with a bandwidth of 11 nm centered at 387 nm. It provides an in-band transmission of more than 93% as well as a suppression of the elastic scattering by ~7 orders of magnitude. The bandpass-filtered optical signal is focused onto the end face of a customized optical fiber bundle (FB) with a numerical aperture (NA) of 0.12 (Fiberguide, US). Its input side is a single 1.5-mm-core diameter fiber, while its output side is composed of seven 0.6-mm-core diameter fibers aligned closely in straight line (for adapting to the 0.8 mm × 7.0 mm geometry of each photosurface of the linear-array photomultiplier tube). A homemade double-grating polychromator (DGP) connects with the fiber output side (the alignment direction of the seven fibers coincides with the grating groove direction).

The DGP has been designed based on the feature of the N_2 Stokes VRR spectra (i.e., 0.12-nm line spacing and ~4.0-nm width centered at ~387 nm). It consists of two separate polychromators with each having a quasi-Littrow configuration. The first one (L1 and G1) performs an initial spectral separation of the bandpass-filtered optical signal. The grating G1 has a groove density of 1200 gr mm^{-1} and blazes at 44.10°operating in the third order. The

#222826 - $15.00 USD Received 11 Sep 2014; revised 13 Oct 2014; accepted 20 Oct 2014; published 3 Nov 2014

lens L1 (focal length = 400 mm and diameter = 100 mm) acts as both collimating and imaging. The other one (L2 and G2) makes a further dispersion and focusing. The grating G2 is of a groove density of 600 gr mm^{-1} and blazes at 54.30°working in the seventh order, while the lens L2 has a focal length of 800 mm and diameter of 130 mm. The adjustment and calibration of the DGP have been made in a similar way as done in building the spectrally resolved Raman water lidar [7]. A system test indicates that the DGP has a reciprocal linear dispersion of 0.12 nm mm^{-1}. A 32-channel linear-array photomultiplier tube (PMT, Hamamatsu H7260A) is used for sampling the N_2 VRR spectral signal via aligning its photosurface precisely on the focal plane of the DGP. Since each channel has a 0.8-mm-wide photosurface (along the linear array direction) and there is 0.2-mm-wide dead area between two adjacent channels, the spectrum sampling interval is just 0.12 nm corresponding to the 1-mm geometric interval between two adjacent channels, which is consistent with the line spacing of the N_2 VRR wing lines. For actual optics alignment, the unresolved Q-branch signals are allocated to the 16th and 17th channels of the 32-channel PMT. In this way, the individual N_2 VRR lines from J = 16 to 2 in the O branch are recorded respectively by the 1st to 15th channels of the linear-array PMT, while the individual lines from J = 0 to 14 in the S branch are detected respectively by the 18th to 32th channels. In other words, the 32-channel PMT samples the N_2 VRR spectra from 384.93 to 388.60 nm with a resolution of 0.12 nm which just equals the line spacing for the majority of the S and O branches. Each channel has a bandwidth of ~0.1 nm (corresponding to 0.8-mm-wide photosurface) which is much larger than the overall broadening (~1.5 pm, by pressure and temperature) of the individual N_2 VRR lines. Hence the detected signal at each of the 32 channels is well represented by the lidar equation (Eq. (4) for a single N_2 VRR line except the 16th and 17th channels where the signal is equal to the intensity sum of the unsolved Q-branch lines over the single-channel bandwidth of ~0.1 nm. Since all the lidar-detected N_2 Stokes VRR lines reside in a wavelength range of ~3.73 nm, the atmospheric transmission $\tau\left(\nu_J^i\right)$ for different Raman frequency shifts is expected to be nearly the same.

At each N_2 Raman channel, the output photons are counted with a bin width of 200 ns corresponding to a 30-m range bin length, and the photon counts from 16500 laser shots are summed to yield a 10-min-integrated data file. The data with a lower time resolution (e.g., 30 min) are obtained simply by cumulating the raw data. The 32-channel photon count data represent a spectrum- and altitude-resolved atmospheric N_2 VRR signal. Such two-dimensional data acquisition is carried out by Licel Multispectral Lidar Detector (Licel, Germany). A PC is employed for overall data acquisition, system control and real-time monitoring of the lidar operation status.

4. Lidar-detected atmospheric N_2 VRR spectra

The lidar equation (Eq. (4), which relates the lidar-detected signal $N\left(\nu_J^i, z\right)$ with the atmospheric N_2 VRR spectra described by the differential backscattering cross section $\sigma^i\left(J,T\right)$ in the O and S branches, can be rewritten in a normalized form as follows:

$$\frac{\sigma^i\left(J,T\right)}{\sigma^S\left(6,T\right)} = \frac{1}{R^i(J)} \frac{N\left(\nu_J^i, z\right)}{N\left(\nu_6^S, z\right)}, \tag{5}$$

where $N\left(\nu_6^S, z\right)$ and $\sigma^S\left(6,T\right)$ are respectively the values of the lidar signal intensity and the differential backscattering cross section for J = 6 in the S branch (the 24th channel). $R^i\left(J\right) = H\left(\nu_J^i\right) / H\left(\nu_6^S\right)$ is the ratio of corresponding two channel transmissions. Equation (5) indicates that the normalized N_2 VRR spectra in the O and S branches $\sigma^i\left(J,T\right) / \sigma^S\left(6,T\right)$

#222826 - $15.00 USD Received 11 Sep 2014; revised 13 Oct 2014; accepted 20 Oct 2014; published 3 Nov 2014

can be obtained from the normalized lidar-detected signal $N(\nu_J^i, z)/N(\nu_6^S, z)$ if the channel transmission ratio $R^i(J)$ is available in advance. For this reason, we have determined the channel ratio values via a laboratory optical measurement. A commercial double-grating (2400 gr mm^{-1}) monochromator (M833, Belarus) together with a white light source (HPLS-30, Thorlabs) were used to yield a wavelength-adjustable monochromatic light. As the entrance and exit slits of the monochromator were both set to be 20 μm, the output monochromatic light had a bandwidth of ~0.02 nm around 386.7 nm. The monochromatic light from the output port of the monochromator was then guided into the DGP via the input side of the FB. The monochromator's output wavelength was set in terms of the line wavelength value (in air) corresponding to each ν_J^i. For a given output wavelength, the 32-channel PMT recorded the signal intensity at the corresponding channel (except the 16th and 17th channels). After subtraction of the background noise and correction of the wavelength-dependent output power of the white light source, the recorded signal intensity at each channel was divided by that at the 24th one. In this way, the channel ratio values were obtained (the partial ratio values are provided in Table 1).

Table 1. Partial channel ratio values from laboratory optical measurement

Channel Number	20	22	24	26	28	30
S-branch Line (J)	2	4	6	8	10	12
$R^S(J)$	1.0880	1.1051	1.0000	0.9935	0.9163	0.8130

Considering Eq. (5), the altitude-dependent atmospheric N_2 Stokes VRR spectra (normalized) can be obtained from our lidar measurement. Figure 3 shows an example measured at Wuhan during 0000-0100 LT on 12 May 2013. Note the original Raman signals of each channel are background-subtracted and then divided by corresponding $R^i(J)$ except

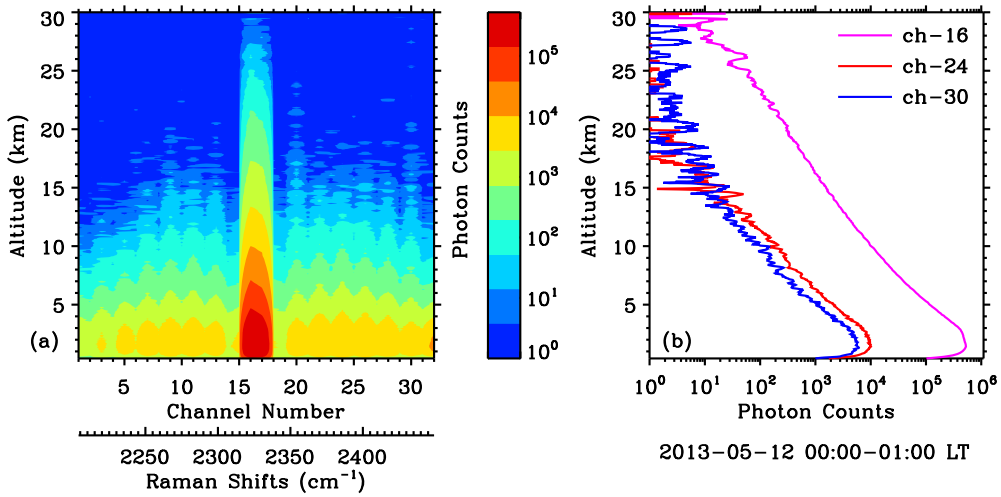

Fig. 3. (a) Altitude-dependent atmospheric N_2 Stokes vibrational-rotational Raman spectra derived from the spectrally resolved Raman lidar measurement at Wuhan during 0000-0100 LT on 12 May 2013. (b) Signal intensity profiles for the 16th (Q branch; magenta), 24th (S branch, J = 6; red) and 30th (S branch, J = 12; blue) channels, respectively.

for the 16th and 17th channels. As seen from Fig. 3(a), the lidar-measured N_2 Stokes VRR spectra are dominated by the unresolved Q-branch lines that are visible up to an altitude of ~30 km. On both sides of the Q branch, the O- and S-branch spectra show a clear-cut sawtooth-like structure which is in agreement with the alternate variation of the N_2 nuclear-

#222826 - $15.00 USD Received 11 Sep 2014; revised 13 Oct 2014; accepted 20 Oct 2014; published 3 Nov 2014

spin statistical weight factor g_N versus even and odd J values. Figure 3(b) plots the lidar signal profiles extracted respectively from the 16th (Q branch), 24th (S branch, J = 6) and 30th (S branch, J = 12) channels. The signal of the summed Q-branch lines at the 16th channel is ~50 times stronger than that of the single S-branch line (J = 6 or 12). Figure 4

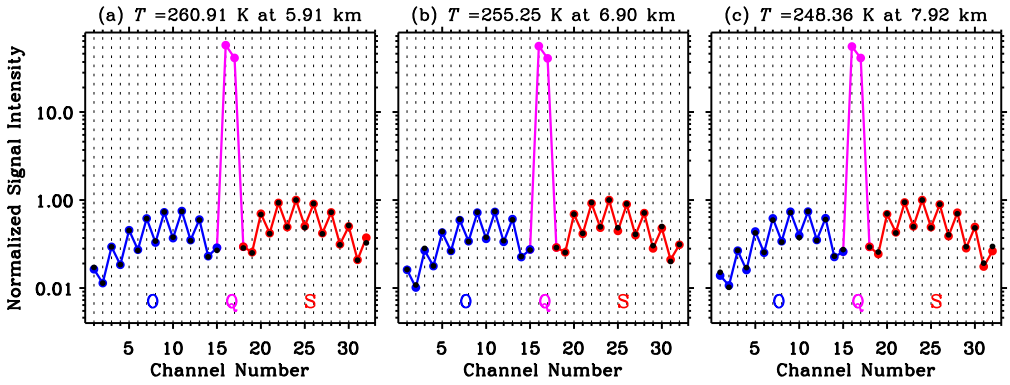

Fig. 4. Atmospheric N_2 Stokes vibrational-rotational Raman spectra measured by the spectrally resolved Raman lidar at altitudes of: (a) 5.91 km; (b) 6.90 km; (c) 7.92 km, respectively. The measurement was performed at Wuhan during 0000-0500 LT on 12 May 2013. For comparison, the theoretically-calculated N_2 Stokes VRR spectra for each given temperature (according to the local radiosonde data) at each altitude in the O and S branches are added (black). Note that the lidar-measured N_2 Stokes VRR spectra in the O (blue) and S (red) branches agree very well (in shape) with the result of the Raman scattering theory.

plots the normalized N_2 VRR spectra at three different altitudes (5.91 km, 6.90 km and 7.92 km respectively with a 90-m altitude resolution) measured during 0000-0500 LT on 12 May 2013 and the theoretically-calculated spectra (black) from Eqs. (1)-(3) for each given temperature (corresponding to a local radiosonde data) at each height. Obviously, the lidar-measured N_2 Stokes VRR spectra in the O (blue) and S (red) branches agree very well (in shape) with the result of the Raman scattering theory. Furthermore, at the other altitudes where the lidar signal-to-noise ratios are sufficiently large, the excellent agreement remains present. Such good agreement allows us to derive the atmospheric temperature profiles via combining two or several N_2 Stokes VRR lines measured by our lidar without requiring a calibration from another temperature data.

5. Temperature retrieval without calibration from another temperature data

5.1 Signal ratio method

Considering two even-J VRR lines (J_1 and J_2) in the S branch, we have the following expression from Eqs. (1)-(5):

$$R = \frac{N\left(\nu_{J_2}^S, z\right)}{N\left(\nu_{J_1}^S, z\right)} = \frac{R^S\left(J_2\right)}{R^S\left(J_1\right)} \exp\left(\frac{a}{T} + b\right). \tag{6}$$

Where

$$a = -\frac{hcB_0}{k}[J_2(J_2+1) - J_1(J_1+1)], \tag{7.1}$$

$$b = \ln\left[\frac{(J_2+1)(J_2+2)(2J_1+3)}{(J_1+1)(J_1+2)(2J_2+3)}\right]. \tag{7.2}$$

#222826 - $15.00 USD Received 11 Sep 2014; revised 13 Oct 2014; accepted 20 Oct 2014; published 3 Nov 2014

The parameters a and b can be figured out via inserting the two selected channel numbers (i.e., J_1 and J_2) and physical constants (B_0, k, h, c) into Eqs. (7.1) and (7.2). Thus, after recalling the relevant channel ratio values $R^S(J_1)$ and $R^S(J_2)$, the temperature profile can be retrieved according to the following relationship:

$$T = f(R) = a / \{\ln\left[\frac{N(\nu^S_{J_2}, z) R^S(J_1)}{N(\nu^S_{J_1}, z) R^S(J_2)}\right] - b\}. \quad (8)$$

Based on Eq. (8) and the lidar data acquired during 0000-0500 LT on 12 May 2013, Fig.

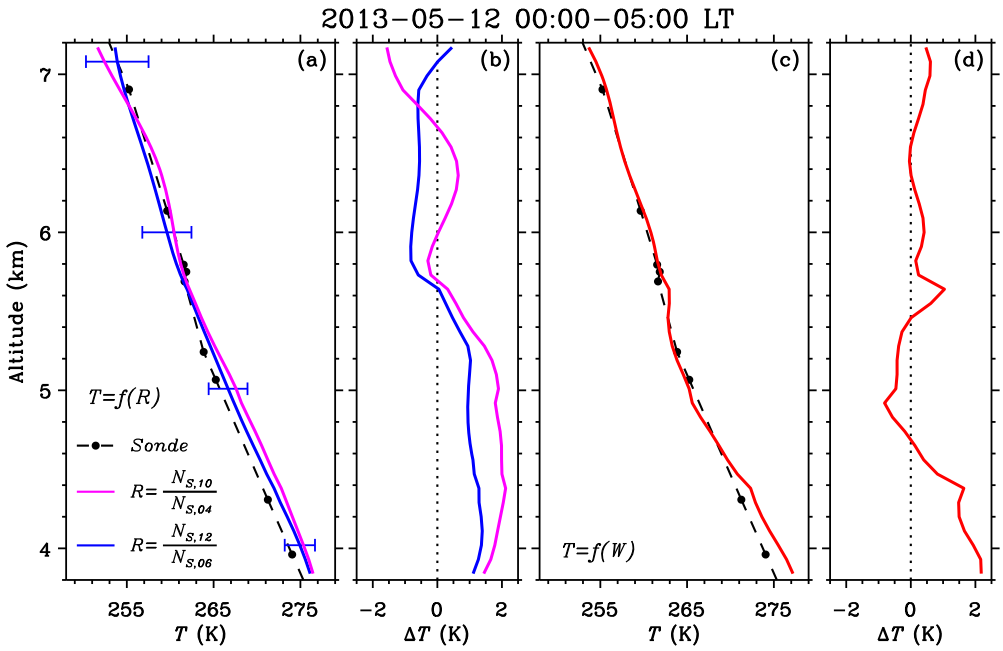

Fig. 5. Temperature profile measured with the spectrally resolved Raman lidar at Wuhan during 0000-0500 LT on 12 May 2013. (a) Temperature profiles obtained by the signal ratio method respectively from the channel pair $J_2 = 12/J_1 = 6$ (blue) and the pair $J_2 = 10/J_1 = 4$ (magenta). For comparison, the radiosonde temperature data at 0800 LT on 12 May 2013 from the Wuhan Weather Station is plotted (black solid circle). (b) Deviations between the lidar-measured temperature and radiosonde data. (c) Temperature profiles from lidar by the envelope method (red) and from radiosonde. (d) Their deviation.

5 plots the two temperature profiles obtained respectively from the channel pair $J_2 = 12/J_1 = 6$ [Fig. 5(a), blue] and the pair $J_2 = 10/J_1 = 4$ [Fig. 5(a), magenta]. As seen from Fig. 5(a), in the altitude range with a sufficient signal-to-noise ratio (3.8-7.0 km), the two profiles show similar behaviors with an absolute deviation less than 1.3 K. It is expected that the deviation is derived from the measurement uncertainty of the channel transmission ratio. Figure 5(a) also gives a comparison between the lidar-measured temperature and the radiosonde data at 0800 LT on 12 May 2013 from the Wuhan Weather Station (~23.4 km northwest of our lidar site). Their algebraic deviation is less than 2.2 K [Fig. 5(b)]. Based on the deviations between the lidar temperature and radiosonde data shown in Fig. 5(b), the measurement error of the channel ratios is estimated to be ~1% or less.

#222826 - $15.00 USD Received 11 Sep 2014; revised 13 Oct 2014; accepted 20 Oct 2014; published 3 Nov 2014

5.2 Spectral envelope method

Figure 1 indicates that the envelope shape of the S- or O-branch spectra (lines) is temperature-dependent. This feature motivates us to develop a new method, designated "spectral envelope method" here, to retrieve atmospheric temperature profile. The first step in the development is to ascertain the functional relation between the envelope shape and temperature. For this purpose, we have calculated according to Eq. (1) the normalized N_2 VRR spectra $\sigma^i(J,T)/\sigma^S(6,T)$ for five selected S-branch lines (J = 2, 4, 6, 8, 10) as the temperature changes from 200 to 300 K with a step of 5 K. Then for each given temperature value the spectral envelope formed by the five VRR lines is fitted using a Gaussian function:

$$I\left(\left|\Delta\tilde{\nu}(J)\right|^S\right)=\frac{\sigma^S(J,T)}{\sigma^S(6,T)}=H\cdot\exp[-\frac{1}{2}\cdot(\frac{\left|\Delta\tilde{\nu}(J)\right|^S-M}{W})^2],\ J=2,4,6,8,10, \quad (9)$$

where $I\left(\left|\Delta\tilde{\nu}(J)\right|^S\right)$ is the normalized line intensity at the Raman frequency shift $\left|\Delta\tilde{\nu}(J)\right|^S$. H, M and W are the fitted Gaussian parameters. The fitting yields numerically the functional relations between the fitted parameters (H, M and W) and temperature. The dotted curve (red) plotted in Fig. 6(a) displays the fitted Gaussian width W versus the given (input) temperature. A best fit, as shown by blue solid circle, to the curve data presented in Fig. 6(a) shows:

$$T=f(W)=A_0\exp[-\frac{1}{2}(\frac{W-A_1}{A_2})^2]+A_3+A_4W, \quad (10)$$

where the fitted parameters A_0 = 221.218, A_1 = 27.074, A_2 = 5.840, A_3 = –1315.970 and A_4 = 41.541. The algebraic deviation between the input and retrieved temperature from the fitted result is less than 0.08 K for the whole temperature range of 200–310 K [Fig. 6(b)]. This indicates that the application of the spectral envelope method enables the retrieved temperatures to perfectly approach the theoretical results with the approximation errors less than 0.08 K in the interested temperature range. According to Eq. (5), the normalized N_2 VRR

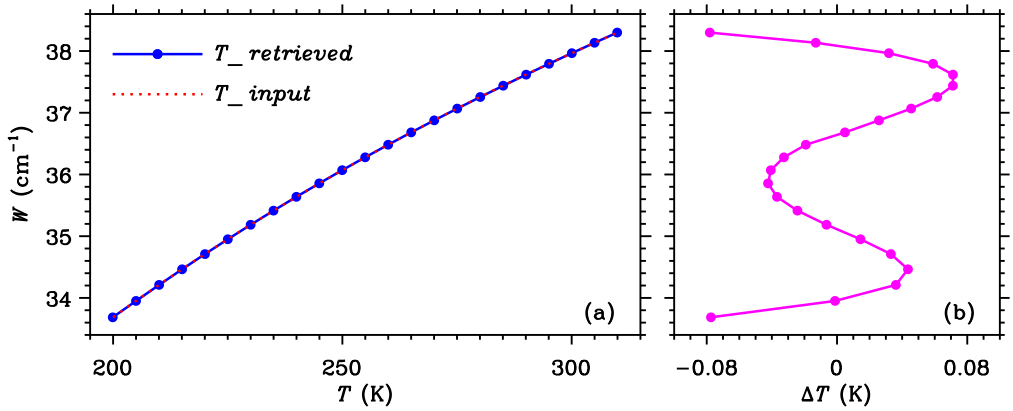

Fig. 6. (a) The input (red) and retrieved (blue) temperature from the fitted result as a function of the fitted Gaussian width W (see text). (b) Algebraic deviation between the input and retrieved temperature (magenta).

spectra $\sigma^S(J,T)/\sigma^S(6,T)$ can be obtained from the normalized lidar signal $N(\nu_J^S,z)/N(\nu_6^S,z)$ since the needed channel ratios $R^S(J)$ are already known. Figure 5(c)

#222826 - $15.00 USD Received 11 Sep 2014; revised 13 Oct 2014; accepted 20 Oct 2014; published 3 Nov 2014

plots the lidar temperature profile retrieved by the envelope method during 0000-0500 LT on 12 May 2013 and the radiosonde temperature at 0800 LT on this day. Their algebraic deviation is less than 2.2 K. In addition, it is noticed that the maximum temperature deviations between the envelope method and the signal ratio method are 1.76 K and 2.61 K respectively for the channel pair $J_2 = 12/J_1 = 6$ and the pair $J_2 = 10/J_1 = 4$ in the 3.8-7.0 km range. The uncertainty of the channel transmission ratio measurement is assumed to be the main source of the deviations.

6. Conclusions and discussion

A spectrally resolved Raman (SRR) lidar has been built to measure atmospheric N_2 Stokes vibrational-rotational Raman (VRR) spectra. The lidar employs an injection-seeded Nd:YAG laser to produce an emission at 354.8 nm and a 1-m telescope to collect the atmospheric backscatter. A self-designed double-grating polychromator (DGP) with a reciprocal linear dispersion of ~0.12 nm mm^{-1} is used for the wavelength separation and suppression of elastic scattering, while a 32-channel linear-array photomultiplier tube (PMT) is utilized for sampling the spectral information. The values of the channel transmission ratio for the 32-channel PMT have been determined by a laboratory optical measurement. The lidar can together measure the individual S-branch line signals from $J = 0$ through 14 and O-branch line signals from $J = 2$ through 16. The lidar-measured Stokes VRR spectra show very good agreement with the theoretically-calculated results. In terms of the S-branch signal ratio from two pairs of selected channels (the channel pair $J_2 = 12/J_1 = 6$ and the pair $J_2 = 10/J_1 = 4$) on an observational night, the atmospheric temperature profiles in the altitude range of 3.8-7.0 km were derived without requiring a calibration from another reference temperature (e.g., radiosonde). The temperature profiles derived respectively from the two different channel pairs show similar behaviors with an algebraic deviation less than 1.3 K. The deviation is presumably due to the measurement uncertainty of the channel transmission ratio. Based on the temperature dependence of the even-J envelope shape of the S-branch lines, a new temperature retrieval approach is proposed that no calibration from reference temperature data is needed. The retrieved temperatures with the spectral envelope method can perfectly approach the theoretical results with approximation errors less than 0.08 K in the interested temperature range (200–310 K). The atmospheric temperature in the altitude range of 3.8-7.0 km was retrieved also by the spectral envelope method on the same observational night and compared with the radiosonde temperature at 0800 LT. Their algebraic deviation was less than 2.2 K.

The uncertainty in the channel transmission ratio measurement affects obviously the accuracy of the retrieved atmospheric temperature. Let us consider the temperature deviation induced due to the uncertainty for the signal ratio method. Given $J_1 = 6$ and $J_2 = 12$, applying the error propagation rule to Eq. (6) yields a temperature deviation expression:

$$\Delta T = \frac{T^2}{a} \frac{\Delta R^S(J=12)}{R^S(J=12)}. \tag{11}$$

According to Eq. (11), a channel ratio uncertainty of 1% would lead to a temperature deviation of 1.2-2.9 K in the 200-310 K temperature range. Its magnitude is comparable to the algebraic deviation between the retrieved temperature and relevant radiosonde temperature, indicating that the temperature measurement error came from the uncertainty in the channel transmission ratio measurement. For the envelope method, the uncertainties distort the spectral shape derived from the lidar signals (see Eq. (5) so that the systematic error would arise in the subsequent temperature retrieval. In practice, simultaneous and co-located observations of the atmospheric temperature with the SRR lidar and radiosonde may help to determine the values of the channel transmission ratio more accurately.

#222826 - $15.00 USD Received 11 Sep 2014; revised 13 Oct 2014; accepted 20 Oct 2014; published 3 Nov 2014

In contrast to the pure rotational Raman backscattering detected by all the existing Raman lidars for profiling atmospheric temperature, our SRR lidar makes use of the relatively-weak N_2 Stokes VRR backscattering. Thus the statistical errors of the present temperature measurement are relatively larger than that of those pure rotational Raman lidars due to its low signal-to-noise ratio (given the same power-aperture products). Several measures can be taken to improve the temperature measurement precision of the SRR lidar. A straightforward way is to enlarge the lidar power-aperture product. In addition, utilizing aurum-coated gratings and optimizing the design of the fiber coupling optics in the lidar system can also improve the lidar efficiency. Noticing a fact that the SRR lidar enables us to retrieve the atmospheric temperature profiles without requiring a calibration from another reference temperature, the relevant lidar technique would be promising in the future tropospheric temperature measurement.

Acknowledgments

This research is supported jointly by the National Natural Science Foundation of China through grants 41327801 and 40221003. The authors would like to thank Yunpeng Zhang, Wei Kong and Miao Weng for technical assistance and support in lidar development.

#222826 - $15.00 USD Received 11 Sep 2014; revised 13 Oct 2014; accepted 20 Oct 2014; published 3 Nov 2014